Eighth International Symposium on Scale Modeling (ISSM-8)
Portland, Oregon, USA, Sept 12-14, 2017

Fire Spread in Chaparral: Comparison of Data with Flame-Mass Loss Relationships[1]

David R. Weise [a,*], Thomas H. Fletcher [b], Shankar Mahalingam [c], Xiangyang Zhou [d], and Lulu Sun [e]

[a] *PSW Research Station, USDA Forest Service, 4955 Canyon Crest Dr., Riverside, CA, USA*
[b] *College of Engineering, Brigham Young University, Provo, UT, USA*
[c] *College of Engineering, The University of Alabama in Huntsville, Huntsville, AL, USA*
[d] *FM Global, MA, USA*
[e] *Embry-Riddle Aeronautical University, Daytona Beach, FL, USA*
[*] E-mail address: *dweise@fs.fed.us*

Abstract

The relationships between flame length, mass loss rate, and the Froude number have become well-established for many different fuels over the past 60 years. Chaparral, a mixture of shrub plants from the Mediterranean climate zone of southwestern North America, represents a fuel type—living plants—that has seldom been included in the development of these relationships. Flame length and mass loss data from single leaves to high bulk density fuel beds similar to wooden cribs were compared to existing correlations for circular and line burner configurations. Fuel moisture content of the fuels ranged up to 100 percent of dry mass, a value outside the range of data used to develop the correlations. Results confirmed the relationship of the Froude number to flame length for these fuels; however, many existing correlations fit the data marginally well. Data from single leaves and circular pans agreed with circular burner correlations better than fuel bed data with line burner correlations. The first evaluation of Albini's thermochemical, wildland fire flame model in chaparral fuels revealed the need for improved data and perhaps changes to the model. Collectively, this data set provided strong support for Byram's correlation of flame length and the square root of mass loss rate. Nelson's effective wind speed related to Byram's convection number significantly improved correlation between the Froude number and flame angle. This Froude number may provide a potential scaling parameter for experiments examining the combined effects of wind and slope.

Nomenclature

- c_p — specific heat (kJ kg^{-1} K^{-1})
- D — characteristic length: leaf diameter (D_l), pan diameter (D_p), flame depth (D_f)
- Fr_{xy} — Froude number based on flame characteristic length x and wind velocity y
- g — gravitational acceleration (m s^{-2})
- H — flame height (m): H_α – calculated from flame angle; H_ϕ - calculated from flame angle and slope angle
- h_c — heat content of fuel, heat of combustion (kJ kg^{-1})
- I — fireline intensity ($h_c m'' r$) (kW m^{-1})
- L — flame length (m)

[1] This manuscript was prepared by a federal government employee as a part of his official duties and is therefore in the public domain and not subject to copyright.

l_y characteristic flame length (*L* or *H*)
m_d oven-dry fuel mass consumed in flaming front (kg)
$\dot{m}_d$ oven-dry mass loss rate (kg s^{-1})
m_d'' oven-dry fuel loading (kg m^{-2})
m_d''' oven-dry bulk density (kg m^{-3})
m_g green fuel mass (includes water) (kg)
$\dot{m}_g$ green fuel mass loss rate (kg s^{-1})
m_g'' green fuel loading (kg m^{-2})
m_w water mass in fuel (kg)
M moisture content of solid fuel (m_w/m_d)
MAE mean absolute error
N mass fraction of unburned fuel in gas mixture; stoichiometric air/fuel mass ratio = kN where k is a fuel specific constant [1]
N_c Byram's convection number: N_c calculated with U, N_{cc} calculated with effective wind speed Uc
NMAE normalized MAE
$\dot{Q}_c$ rate of heat release (kW)
$\dot{Q}_l$ rate of heat release per unit length (kW m^{-1})
R rate of spread of line fire (m s^{-1})
r Pearson product moment correlation coefficient, r^2 is the coefficient of determination
RMSE root mean squared error
T absolute temperature (K)
U horizontal wind velocity (m s^{-1})
U_c effective wind velocity combining U and ϕ [2] (m s^{-1})
U_x characteristic wind velocity (U or U_c)
V vertical velocity in flat flame burner (m s^{-1})

α angle of flame from vertical $\left[\cos^{-1}\left(H/L\right)\right]$
β fuel gas mass produced per unit of fuel bed mass loss
γ linear regression coefficients
η,ζ entrainment coefficients; ζ is denoted α in [58]
ϕ angle between horizontal and axis of tilted fuel bed (slope)
ν kinematic viscosity of air (m^2 s^{-1})
ρ density (kg m^{-3})
ρ_c measure of model fit for circular regression
χ^2 $\sum\frac{\left(observed - predicted\right)^2}{predicted}$, chi-squared statistic

Introduction

The flame of a wildland fire is the visible manifestation of combustion processes in wildland fuels. This primarily turbulent diffusion flame is a heat source affecting its immediate surroundings. Energy transferred from a flame to the environment can cause a variety of fire effects on plants, animals, soil, water, air and cultural resources [3–8]. Flame size is used as a metric for fire suppression action and firefighter safety zone size [9–11]. Perhaps because of the importance of a fire's flame to man, there is a large body of knowledge related to flame structure and there has been a significant effort deriving flame models and developing correlative relationships with other fire characteristics [e.g. 12]. In the United States, Byram was a pioneer in wildland fire research and contributed in many areas including the development of scaling laws [13, 14]. In addition to studying fire whirls with scaled experiments [15], he studied the fire plume in crossflow and developed a dimensionless ratio of the power of wind and power of the fire (convection number N_c, Eq. (1)[16]) as a measure of the potential for a wildland fire to "blow up". N_c was subsequently shown to be proportional to a Froude number [17–21] based on flame height (U^2/gH). Byram used ambient atmospheric properties ρ and c_p in this derivation. Over 50 years of experiments and modeling have established the scaling of H with the Froude number for axisymmetric and linear fires using burner diameter or flame depth as the characteristic length (D), respectively [18, 22–24]. Flame data from wildland fuels have been included in this development; however, the wildland fuels have typically been dead fuels and not live fuels. Nelson [17] cited examples where N_c had been applied to spotting and crown fire spread – crown fires by definition typically spread through live fuels. Recent work has examined and modeled Froude-based flame geometric relationships in European shrub lands similar to chaparral [25–28].

$$N_c = 2gI \Big/ \left[\rho_a c_p T \left(U - R \right)^3 \right] \quad (1)$$

Wildland fuels include living vegetation and the dead foliar and wood components that are either retained on the plant or deposited on the ground. While the emphasis on wildland fuels has been on the dead component, fires burning in living vegetation are a significant portion of the wildland fires which occur worldwide. In regions of the world where Mediterranean climates occur, wildland fuel often consist of shrubs which can exhibit significant fire behavior. Shrub fuels are not restricted to Mediterranean regions and include sagebrush in the interior western United States and southern rough in the southeastern U.S. Chaparral is a plant community containing many species of shrubs that grow in the Mediterranean climate region of the U.S. located in California and northern Baja Mexico.

As part of a larger program studying fire spread mechanisms in live fuels with an emphasis on chaparral vegetation [29], experimental work has been conducted at Brigham Young University (BYU), the University of California at Riverside (UCR) and the USDA Forest Service Forest Fire Laboratory (FFL) in Riverside, CA, USA since 2001. Work at BYU developed a flame angle (α) – Froude number correlation for single leaves in cross-flow from a variety of shrubs [30] and work at UCR examined the relationship between H and heat release rate for pans of live and dead foliage and branches from chaparral species [31]. While fire spread experiments have been conducted at both the fuel bed and field scale in chaparral fuels [32, 33], the relationships between flame characteristics and heat release or mass loss have not been explored extensively. This paper compares laboratory data from single leaf to fuel bed scale experiments with several existing relationships to determine the feasibility of scaling the laboratory results to the field scale. Because high water content is an important characteristic of live fuels, the mass loss rate used in this study is $\dot{m}_g$, not $\dot{m}_d$.

Methods

Experimental setups

Material for all chaparral experiments at BYU, UCR, and FFL were collected at the North Mountain Experimental Area located 50 km east of Riverside, CA at an elevation of 1160 m. Samples of chaparral were cut and sent by express mail to Utah. Four species were examined: Eastwood's manzanita (*Arctostaphylos glandulosa* Eastw.), scrub oak (*Quercus berberidifolia* Liebm.), hoaryleaf ceanothus (*Ceanothus crassifolius* Torr.) and chamise (*Adenostoma* *fasciculatum* Hook. & Arn.) representing the range of physical characteristics for species comprising chaparral. Flame height (*H*) and mass loss rate ($\dot{m}$) data in the present paper were estimated during the steady burning period of each set of experiments. The mass loss data recorded in all experiments included water mass ($\dot{m}_g$). Our previous work has shown that live fuels such as leaves contain significant amounts of water at the time of ignition [34, 35]. In the BYU and UCR experiments, wind velocity U = 0 and slope angle ϕ = 0. These data were collected prior to the work reported in [30].

The experimental apparatus at BYU was designed to closely resemble the conditions of a forest fire flame front [36]. The fuel sample (a leaf or branch (chamise)) was attached to a stationary horizontal rod connected to a cantilever-type mass balance. A flat-flame burner (FFB) was positioned on a moveable platform to simulate the flame front. The platform was pulled at a constant velocity toward the fuel sample. The post-flame gases from the FFB provided heat transfer by convection. The post-flame gas vertical velocity *V* was 1-2 m s^{-1} and the gas temperature was 1000 °C. Using leaf diameter (D_l) as the characteristic dimension *D* resulted in the Reynolds number (VD/ν) ranging from 46 to 726 indicating forced convection with laminar flow. A video camera recorded the burning foliage. *H* was determined by averaging measurements of maximum *H* from still images taken from the video. Even though the work at BYU included other species common to Utah and the southern U.S. [34, 37], we used only data from chaparral species in this study. Color imagery of some of the combustion behavior observed during the heating, ignition and burning of the moist leaves revealed interesting phenomenon such as bursting and boiling not typically observed in dead fuels ([34, 38]).

At UCR circular pans of green and dry chaparral fuels were placed on an electronic scale and ignited [31]. Pan diameters (D_p) of 0.3, 0.45, and 0.6 m and a constant dry fuel loading m'' of 2.12 kg m^{-2} were used. A constant pan depth of 0.2 m resulted in constant bulk density m''' of 10.6 kg m^{-3}. Each pan was ignited using an alcohol-soaked paper towel placed in the bottom of the pan under the chaparral fuel. A height marker placed adjacent to the scale provided a reference scale. A video camera and thermal infrared camera recorded each experiment. *H* was determined by averaging measurements of maximum *H* from still images taken from the video [31] after the alcohol and paper were consumed. For these experiments $D = D_p$.

The effects of wind (*U*), fuel moisture content (*M*), fuel bed height and slope angle (ϕ) on flame propagation in live fuels were studied at FFL (Fig. 1) using fuel beds (2.0 m long × 1.0 m wide × various depths) constructed of live branch material < 0.64 cm and foliage material [32, 33]. The fuel beds were elevated above the surface of a tilting platform by 0.4 m to simulate an aerial fuel. Air could be entrained from the ends of fuel beds; metal sheeting prevented air entrainment from the sides to reduce the curvature of the flame front and simulate a line fire. Plant material was generally collected in the morning so as to minimize moisture loss through transpiration. Dead fuel was removed to the extent possible. Dry bulk density m_d''' ranged from 6.26 to 14.01 kg m^{-3}; reported natural bulk density of chaparral canopies ranged from 0.4 to 3 kg m^{-3} [40]--values significantly lower. The slope $\left(100\tan\phi\right)$ of the fuel beds ranged from -60 to 70 percent where negative values indicate fire spread downhill [19, 39]. A fuel bed was ignited along the 1 m side with an ignition zone of 50 cm depth. Between 0.3 and 0.4 kg of excelsior and a small amount of isopropyl alcohol were added uniformly in the ignition zone to initiate and sustain the ignition. A video camera recorded each experiment and several images during the steady burning phase (near 1 m) were digitized to measure flame characteristics including height, length, depth, and angle. Mass loss rate $\dot{m}_g$ was estimated by combining green fuel loading $m_g^{"}$, rate of spread R and flame depth (D_f) (Eq. (2)). For the fuel bed data $D = D_f$.

$$\dot{m}_g = m_g^{"} R D_f \tag{2}$$

Flame relations

The relationship between mass loss rate and flame length was examined initially. Scatterplots suggested potential statistical relationships which we fit using linear and nonlinear regression. We compared observations with predictions from the empirical models of Byram [16] (Eq. (3)), Fons et al. [41] (Eq.(4)) and Thomas [42] (Eq.(5)) as reported in [18, eq. 40-42]. The sources of these equations did not specify that mass was oven-dry mass; however, that may have been an unwritten assumption. We used the χ^2 statistic as a measure of the goodness of fit between observed and predicted flame length [43]. In order to evaluate the application of Eq. (3)-(10) to flame characteristics from live fuels, we used $\dot{m}_g$ for $\dot{m}$.

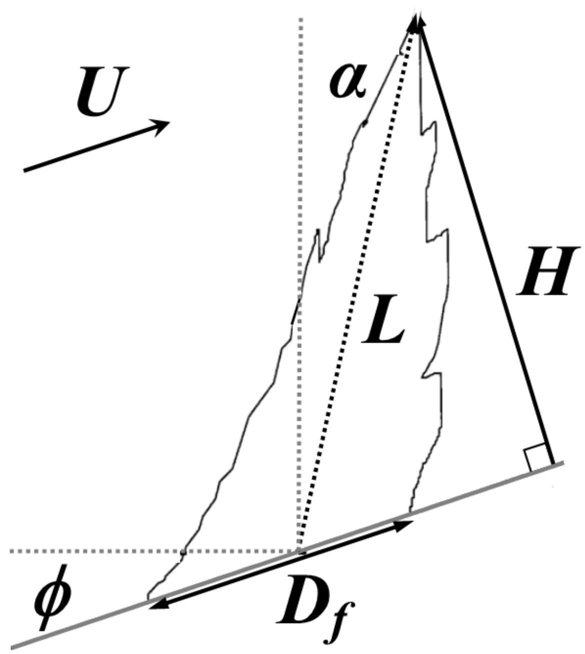

Fig. 1. Components of the diffusion flame resulting from the burning of wildland fuels for a fire spreading on sloped ground (ϕ).

$$L = 3.22\dot{m}^{0.46} \tag{3}$$

$$L = 3.13\dot{m}^{2/3} \tag{4}$$

$$L = 3.94\dot{m}^{2/3} \tag{5}$$

For wind-driven fires on flat ground $(\phi = 0)$, Albini [18] presented correlations for flame dimensions from Thomas [20, eq. 7i, 7ii] (Eq.(6)) and reported good agreement between observed and predicted of H and α for dead pine needle fuels using modelled thermochemical properties [1]. Since these correlations resulted from fire spread in wooden cribs with wind we used fuel bed data with $U = 2$ m s^{-1} to evaluate these correlations.

$$\begin{aligned} H &= 101\dot{m}U^{-0.74}D^{-0.13} \\ L &= 10.25\dot{m}^{0.86}U^{-0.22}D^{-0.18} \\ \alpha &= \cos^{-1}\left(4.38\dot{m}^{0.14}U^{-0.78}D^{0.18}\right) \end{aligned} \tag{6}$$

We also compared the fuel bed data to Albini's wind-driven flame model [18] (Eq.(7)). Since modeling results have shown that the presence of water vapor in the combustion gas mixture reduced maximum temperature of the flame and reactions were quenched when the water mole fraction exceeded 0.65 [44], we incorporated the effect of M on the fuel gas production ratio β and the stoichiometric air/fuel ratio N using the curves for manzanita and chamise foliage [1]. To estimate we fit a linear regression model of the following form $\beta, N = \gamma_0 + \gamma_1 M + \gamma_2 M^2$ using visually-estimated data points from the published curves. This model has an additional term when compared to the simple linear equations for white and ponderosa pines [18]. Albini [18] assumed a straight line relationship for M over the range of 0.02 to 0.15 [45, 46]. M of the chaparral fuel beds ranged from 0.26 to 0.91; Albini's curves [1] contain significant curvature over this range. Linear correlation between observed and predicted flame dimensions was estimated using the Pearson product moment correlation coefficient (r) [47].

$$\begin{aligned} H &= 122N\beta\dot{m}/U \\ \alpha &= \tan^{-1}\left(0.0036U/\sqrt{H}\right) \end{aligned} \tag{7}$$

Circular regression tested the strength of the relationship between observed and predicted flame angle (α) [48, 49] (Eq.(8)). A measure ρ_c, similar in interpretation as the coefficient of determination r^2 in ordinary least squares analysis, described the goodness of fit of the circular regression.

$$\cos(\alpha_{Obs}) = \gamma_0^c + \sum_{k=1}^{m} \gamma_{ck}^c \cos(k\alpha_P) + \gamma_{sk}^c \sin(k\alpha_P)$$
$$\sin(\alpha_{Obs}) = \gamma_0^s + \sum_{k=1}^{m} \gamma_{ck}^s \cos(k\alpha_P) + \gamma_{sk}^s \sin(k\alpha_P) \quad (8)$$

where subscript *Obs* and *P* indicate observed and predicted, superscripts *s* and *c* are related to sin and cos of α_O, subscript *ck* and *sk* relate to sin and cos of α_7.

For circular burners and square cribs, *H* has been correlated with the heat release rate ($\dot{Q}_c$) by Eq. (9) [12, 22]. In these configurations, the characteristic length *D* is burner diameter or length. For a line burner (or line fire) with turbulent flames and rate of heat release greater than 30 kW/m, heat release rate ($\dot{Q}_l$) and *H* have been correlated by Eq. (10) [23]. Note that Byram's fireline intensity *I* [51] which is calculated for a spreading fire has the same units as $\dot{Q}_l$. We evaluated the fit of Eq. 8 to the leaf and pan data and the fit of Eq. 9 to the fuel bed data assuming air properties at 25 °C, a low heat of combustion (h_c) of 16.77 and 16.31 kJ/g for chamise and manzanita, respectively, and $\dot{Q} = h_c \dot{m}$ [1,31].

$$H/D = Q_c^* = \frac{\dot{Q}_c}{\rho_\infty c_p T_\infty \sqrt{gD}\, D^2} = \frac{h_c \dot{m}}{\rho_\infty c_p T_\infty \sqrt{gD}\, D^2} \quad (9)$$

$$H/D = 3.46 \dot{Q}_l^{*2/3} = 3.46 \left(\frac{\dot{Q}_l}{\rho c_p T \sqrt{gD}\, D} \right)^{2/3} = 3.46 \left(\frac{I}{\rho c_p T \sqrt{gD}\, D} \right)^{2/3} \quad (10)$$

All of the correlations presented above assume a horizontal orientation of the fuel bed $\phi = 0$. While extensive work has examined fire spread on vertical surfaces, this seldom, if ever occurs in wildland fires. Recent work by Nelson [52] applied to the results reported by [26] presented Froude numbers modified to take into account the combined effects of *U* and ϕ using an effective wind speed $U_c = U + \left(2gI/\rho c_p T\right)^{1/3} \sin(\phi)$ [2]. Fig. 1 reflects this geometry. The relationship between various Froude numbers based on *L*, H_α and H_ϕ coupled with *U* and U_c and flame angle was examined using the fuel bed data and the general form of the Froude number $Fr_{xy} = (U_x - R)^2 / gl_y$. Typically the Froude number has been related to the tangent of the flame angle using a simple linear regression of the form $\tan(\theta) = \gamma_0 + \gamma_1 Fr_{xy}$ where $\theta = \alpha + \phi$. Analysis of circular data has advanced to the point that linear-circular regression can be readily used as well. Linear-circular regression relates a circular variable to linear variables through a link function involving $\tan^{-1}$. We verified that the fitted values from both regression approaches were linearly related (straight-line relationship) and present the results for the linear-circular regression of the model $\theta = \gamma_0 + \gamma_1 Fr_{xy}$. Residuals from the fitted regressions were compared by the MAE (mean absolute error), NMAE (normalized MAE) and RMSE (root mean squared error) [54]. Statistical analysis and graphing were performed using R version 3.4.0 [50].

Results and discussion

Ninety-eight pan experiments were conducted with no imposed flow, 123 leaf experiments were conducted in laminar vertical flow of 1-2 m/s imposed by buoyancy above the flat flame burner and 58 bed experiments were conducted with no wind and cross flow of 2 m/s for a total of 279 observations. A plot (Fig. 2) of the flame length data against the untransformed mass loss rate for chaparral fuels suggested a significant relationship and the possibility of developing a correlation between the two variables. Using nonlinear regression, we fit the equation $L = 0.6\dot{m}_g^{0.34}$ to the leaf, pan, and fuel bed data which statistically is the same as $L = 0.6\dot{m}_g^{1/3}$. We previously reported a significant correlation between mass loss rate and heat release rate with flame length for the pan data [31]. For leaf data for a wide variety of species, flame height was a power function of mass loss; however, the model did not account for much of the variability [53]. For the fuel bed data, we previously fit a similar nonlinear equation ($L = 0.2I^{0.34}$) relating flame length to fireline intensity based on $m_d^{"}$ [54]. In the present study a log-log plot revealed a significant linear relationship $\log(L) = -0.866 + 0.475\log(\dot{m}_g)$ (Fig. 2). The leaf flames were primarily laminar while the pan and bed tests produced turbulent flames. Experiments at field scale where flame lengths are larger by an order of magnitude (10s of meters) could prove more enlightening.

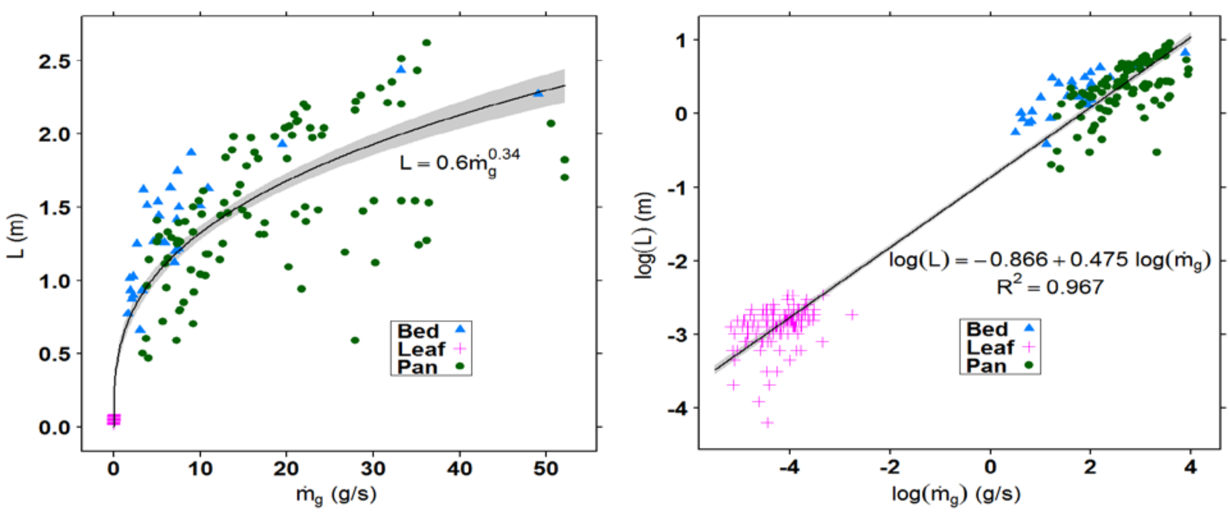

Fig. 2. Regression models relating flame length (L) and mass loss rate ($\dot{m}_g$) fitted using nonlinear least squares (left) and ordinary least squares (right). The grey band illustrates the 95 percent confidence interval for the nonlinear least squares fit.

Empirical correlations

For the wind only data, of the three empirical flame equations (Eq. 3-5), Byram's fit the data best with the smallest χ^2 statistically significant statistic; the χ^2 values were 1894, 1319, and 451 for

Thomas, Fons, and Byram, respectively (Fig. 3). Thomas and Fons tended to over predict the data due to the greater exponent (2/3) which Albini [18] reported for his data. In [41, 42], *M* for the wooden cribs ranged from 0.04 to 0.16 – a typical range for dead fuels that burn. *M* for the chaparral fuels ranged from 0.26 to 1.00 – the upper value is within the upper value for the annual moisture cycle in these live chaparral fuels. Note the close agreement between Byram's exponent and the exponent of the transformed log-log fitted equation (0.46 versus 0.48). Changing units and transforming the fitted log-log equation (Fig. 2) resulted in $L = 3.18\dot{m}_g^{0.48}$, a result very similar to Eq. (3). While the regression equation relating observed and predicted *H* (from Eq. 6) was statistically significant (Fig. 4), Eq. 6 consistently underestimated *H* generally and consistently predicted larger α for the chaparral fuel beds (not shown). The prediction of larger α by Eq. (6) is consistent with results reported in [18].

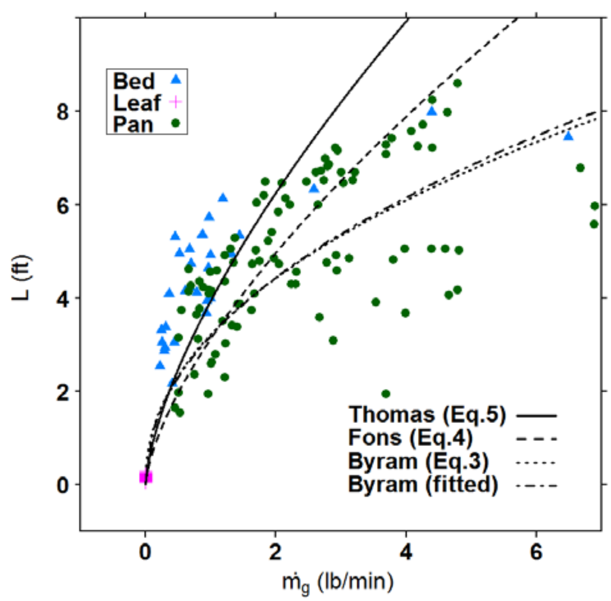

Fig. 3. Comparison of three published flame length-mass loss equations and a fitted equation with data for chaparral fuels ranging from a single leaf to a 2 m fuel bed (Eq. (3)-(5)).

Albini flame model (eq.(7))

The fitted regressions of β and *N* for chamise and greenleaf manzanita (*Arctostaphylos patula* Greene) are summarized in Table 1. While the regressions did not account for all of the variation in the data, they captured most of the variability and can be used in other applications where it may be desirable to predict thermochemical properties of live fuels such as in [55]. The simplified form of Albini's flame model for wind-driven fires also significantly underestimated *H* (Fig. 4). The under prediction was greater than Eq. (6). While $\dot{m}_g$ was numerically greater than $\dot{m}_d$ which would numerically increase *H* and β, in actuality the stoichiometric air/fuel gas ratio is decreased due to the presence of water vapor from fuel moisture *M*. The use of β and *N* for green chaparral fuels resulted in α closer to the observed values than Thomas's equation; however, the predictions were still statistically different from the observed data. The over prediction of α is a direct result of the under prediction of *H*. Predicted mean α was 60° which was significantly different from the observed mean α of 18°. While Eq. (7) over predicted α, circular regression indicated a strong linear relationship between the predicted and observed flame angles (Fig. 5). The measure of model fit ρ_c for the order 1 model was high (0.997) (Table 2); however, statistical testing indicated that the order 2 coefficients were significantly different from zero. While the fit of the order 2 model was only slightly better (0.999), the improvement in the model can be seen in Fig. 5.

Table 1. Summary of fitted regression models to estimate fuel gas mass (β) and the stoichiometric air/fuel mass ratio for fuel gas (N) using Albini's thermochemical model **[**1**]**. The general regression model was $Property = \gamma_0 + \gamma_1 M + \gamma_2 M^2$ where M is moisture content.

Property	Species	γ_0	γ_1	γ_2	r^2
β	chamise	1.873	0.0207	-1.0E-4	0.925
	manzanita	1.938	0.0168	-6.7E-5	0.876
N	chamise	2.357	-0.0484	2.9E-4	0.944
	manzanita	2.235	-0.0462	2.8E-4	0.940

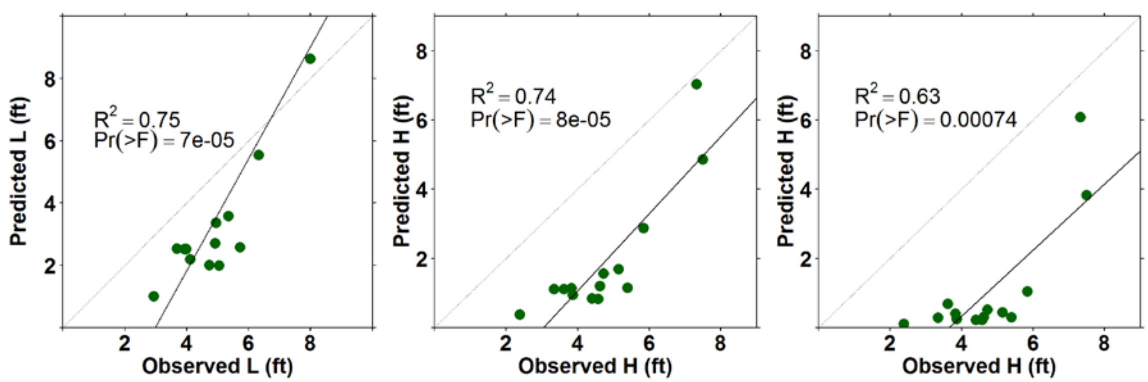

Fig. 4. Comparison of observed and predicted flame sizes using Albini's approximations of Thomas' correlations (Eq. 6) for L (left) and H (center) and Albini's flame model (Eq.(7)) for H (right) in wind for fuel bed data.

Table 2. Coefficients of circular regression relating observed flame angle α with α predicted using Eq. (7). The coefficients are used in Eq. (8) to predict the sin and cos components of α.

Equation	Order (m)	Intercept (γ_0)	γ_{c1}	γ_{c2}	γ_{s1}	γ_{s2}	ρ_c
$\cos(\alpha_O)$	1	0.328	0.455		0.460		0.997
	2	-16.738	17.808	-0.448	16.471	-6.598	0.999
$\sin(\alpha_O)$	1	1.236	-0.751		-0.629		
	2	16.017	-21.824	4.093	-10.238	7.093	

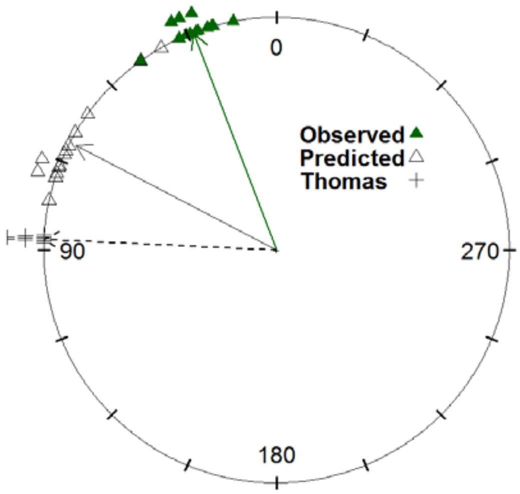

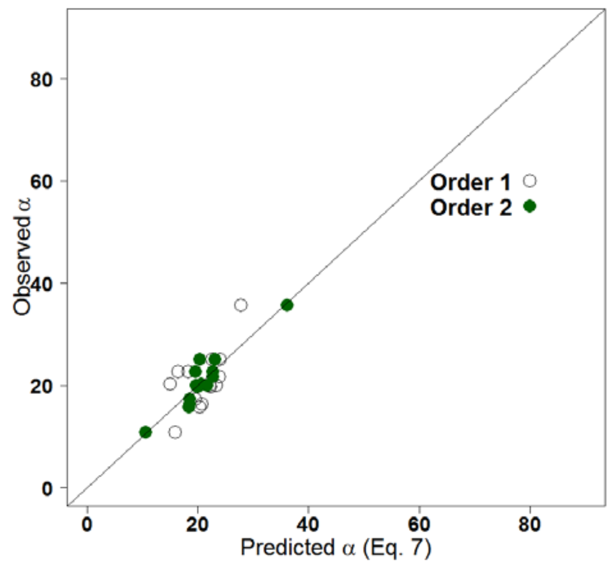

Fig. 5. Comparison of flame angle α predicted by Albini's flame model (Eq.(7)) with observed data (left). The arrows indicate the means of the observed and predicted angles. Predictions of α from Eq. (6) are included for comparison (+). Comparison of circular regression fitted values versus observed α for a 1st and 2nd order model.

Heat release rate $\left(\dot{Q}_c, \dot{Q}_l\right)$

For the pan fires, the data fell close to the visually estimated correlation derived by Zukoski [56] (Fig. 6). The leaf fires generally fell below this correlation. Zukoski [56] identified 5 regions defined by $\dot{Q}_c$. Region II was defined as $0.1 < \dot{Q}_c < 1$ and Region III was defined as $1 < \dot{Q}_c < 700$. The pan fires and some of the leaf fires fell in Region II; the remainder of the leaf fires fell into Region III. In Region III, buoyancy dominates and the flame height depends primarily on heat release rate. In Region II, flame height depends on diameter and heat release rate. A correlation based on LES simulations of a statistically-stationary fire burning in an isolated chamise shrub for a range of bulk densities [60, 61] was included in Fig. 6 for comparison with the leaf and pan data. All pan and leaf data fell below this correlation as well. A strong linear relationship between height and heat release is evident for both the pan and leaf data. For the pan and leaf data, $L = H$.

There was no evidence of a linear relationship between $\dot{Q}_l$ and L or H (Fig. 6, right) for the fuel beds that spread on level ground ($\phi = 0$) as indicated by the non-significant F-statistics. For these data, $H_\alpha = L\cos(\alpha)$. When H was calculated as $H_\phi = L\cos(\alpha + \phi)$ to adjust for slope angle [52] and the data for both level and upslope spread were regressed on $\dot{Q}_l$, a significant regression resulted (dashed line). The fitted model (dashed line) accounted for a small portion of the observed variation ($R^2 = 0.10$). The data for the level fuel beds were clustered around the solid line that represented the estimated upper bound of the correlation for a line fire [57]. $\dot{Q}_l$ and I ranged from 65 to 2452 kW/m.

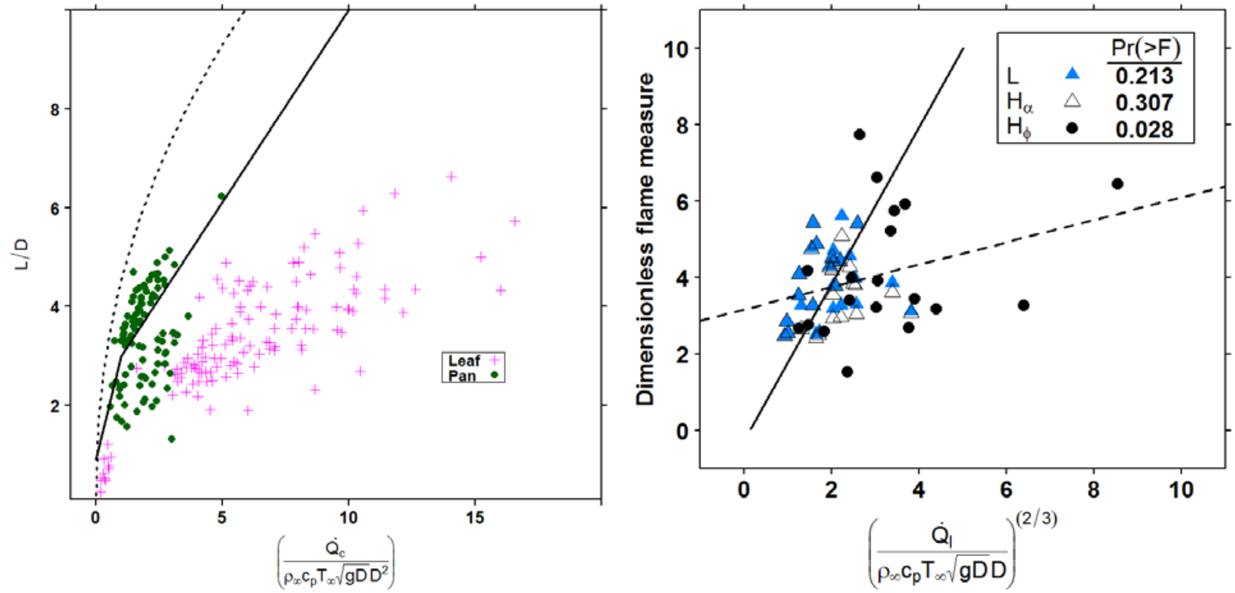

Fig. 6. Relationship between scaled flame height and dimensionless heat release rate for circular (left, Eq.(9)) and line (right, Eq.(10)) fires in chaparral fuels. In the left plot, a visually estimated line for Zukoski's correlation [56] is included (solid) as is the correlation (dotted) developed for a statistically-stationary fire burning in a chamise shrub [60]. In the right plot, a solid line for the estimated line fire bound is included [12]..

Byram's N_c and Froude numbers

For the 19 fuel beds used in the comparison with Albini's flame model (Eq.(7)), the convection number N_c calculated with U ranged from 0.94 to 7.34. Based on N_c, these data fell into the intermediate region defined in [52] where heating prior to ignition is a mixture of convection and radiation. Of the 19 fires, 5 spread on slopes ranging from 26.8 to 40 percent $\left(15^\circ \le \phi \le 22^\circ\right)$. Since $N_c < 10$ for these fires, we regressed $\tan(\alpha+\phi)$ against $N_c^{-1/2}$ and $N_{cc}^{-1/2}$ and forced the curve though 0 [58]. The regression for $N_c^{-1/2}$ was not significant ($\Pr > F = 0.73$) as can be seen in Fig. 7. The regression for convection number based on effective wind speed $\left(N_{cc}^{-1/2}\right)$ was significant and accounted for 91% of the total variation (uncorrected for the mean). The usual Pearson r^2 provides spurious information for regression through the origin models [59] so an alternative r^2 was calculated as in [58]. The slope estimate from the chaparral data (0.609) yielded an entrainment constant η = 0.19 [58, eq. 23] which differed from Nelson's η = 0.71 for fuel beds of pine litter and palmetto fronds [58]. $\mathrm{Tan}(\alpha+\phi)$ was also regressed against $N_{cc}^{-1/3}$ (Fig. 7). This regression was also significant and accounted for 91% of the total variation. Mean absolute error between observed and predicted values was similar for the 2 N_{cc} models. The slope estimate for chaparral of 0.548 produced an estimate of the entrainment constant ζ = 0.15 which also differed from Nelson's ζ = 0.55 [58]. One important difference between the fuel beds used in [58] and the chaparral fuel beds in the present study is that the pine needle-palmetto fuel beds were contiguous with the ground which restricted air flow from underneath the burning vegetation. The chaparral fuel beds were elevated; lateral entrainment was blocked, but air flow under the fuel bed was possible. Model simulations demonstrated this flow was significant for fires spreading up slopes [39] which would potentially alter the entrainment constants for these fires.

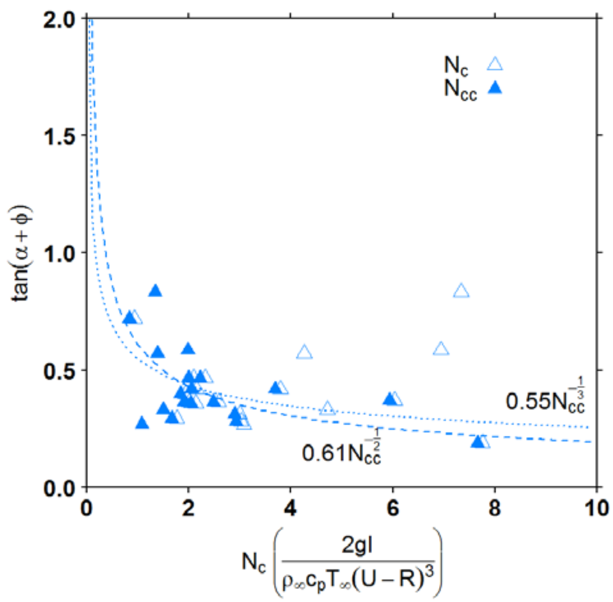

Fig. 7. Relationship between flame angle and Byram's convection number calculated using 2 different wind velocities. N_c was calculated using wind velocity U and N_{cc} was calculated using effective wind velocity U_c. The fitted curves were developed using N_{cc}. The x-coordinates for N_{cc} have been dithered (shifted slightly) so that overlapping points can be seen.

Six Froude numbers were calculated based on L, H_α, and H_ϕ with U and U_c: Fr_{LU}, Fr_{Lc}, $Fr_{H\alpha}$, Fr_{Hc}, $Fr_{H\phi}$, $Fr_{H\phi c}$. The Froude numbers all occurred in the range $0 \le Fr_{xy} \le 1$; Froude numbers reported for fires in shrub fuels in France also fell within this range [28]. For the shrub fuel beds in the present study based on the t-test statistic, all slope coefficients for the Froude numbers were significantly different from 0 with probability values < 4E-7 (Table 3). Use of the slope correction (subscript c) improved the fit of all regression as indicated by MAE, NMAE and RMSE measures. On average, the NMAE was reduced by 0.07 (7%). The error metrics for Froude numbers based on L were slightly larger than the error measures for H-based Froude numbers (Fig. 8); however, when normalized by the mean flame angle, we observed little difference in the predictive capability for flame angle between the Froude numbers based on L versus H.

For the leaf and pan data, there is strong support for the well-established Froude scaling for these live fuels using the mass loss rate that includes water. It may be possible to reduce the scatter in the data by identifying the relationship or characteristic length that will improve the correlation. Fuel moisture, fuel particle shape and thermochemical characteristics are potential variables. The fuel bed data includes non-zero slope and wind effects which may contribute to the scatter. Nelson's recent formulation of Froude numbers for fires spreading under wind and slope effects [52] improved the correlation with flame angle; Froude numbers based on flame height generally performed better. This limited test coupled with previous results on the effectiveness of U_c in dead fuels [19] suggests that a Froude number based on U_c might be useful scaling parameter for experiments examining wind and slope effects on fire behavior. The ability to scale results from these smaller experiments to full-scale wildland fires remains to be demonstrated. Factors such as fuel moisture and varying fuel particle shape are perhaps characteristics unique to wildland fire. Most correlations appear to be developed from fuels where free water in the fuel is not an important component.

Table 3. Summary of circular-linear regressions of flame angle with various Froude numbers. Mean absolute error (MAE) and root mean squared error (RMSE) expressed in radians, normalized MAE (NMAE) is a proportion.

Fr_{xy}	Effective wind velocity	Intercept (γ_0)	γ_1	MAE	NMAE	RMSE
Fr_{LU}		0.263	0.249	0.090	0.231	0.118
Fr_{Lc}	Y	0.125	0.414	0.064	0.163	0.078
$Fr_{H\alpha}$		0.261	0.234	0.088	0.224	0.115
Fr_{Hc}	Y	0.114	0.405	0.057	0.147	0.069
$Fr_{H\phi}$		0.210	0.319	0.084	0.216	0.109
$Fr_{H\phi c}$	Y	0.158	0.325	0.059	0.150	0.069

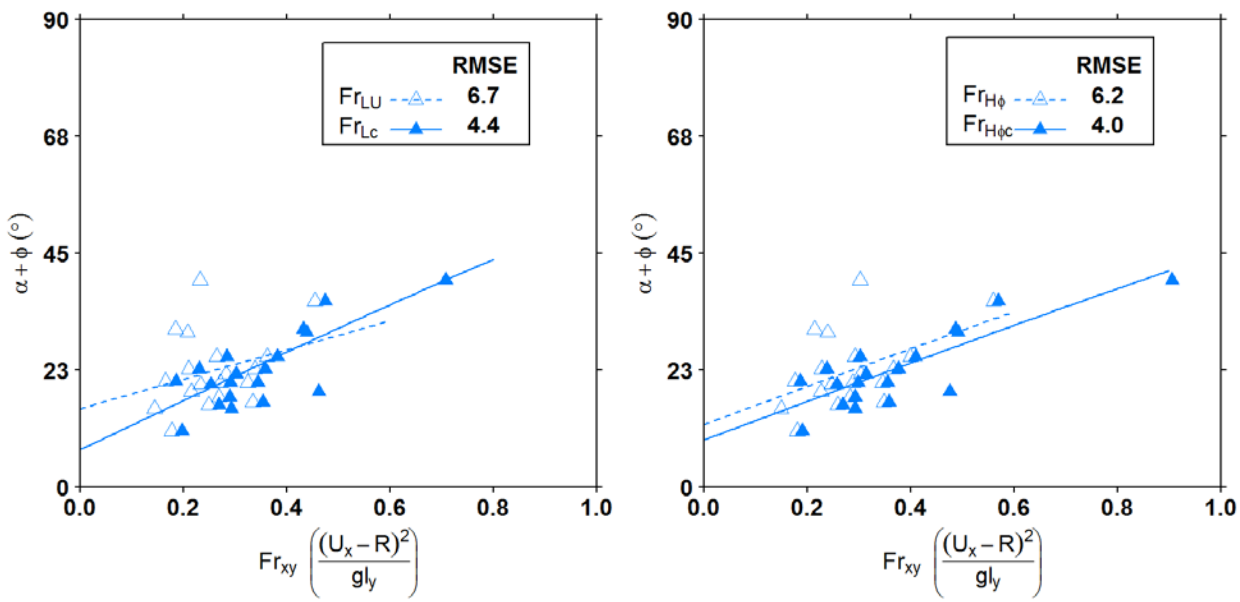

Fig. 8. Correlation between flame angle α corrected for slope ϕ and Froude numbers based on flame length L (left) and flame height H corrected for slope (right). Each plot illustrates the impact of effective wind speed U_c [2] on the fitted regressions. The x-coordinate of the Froude numbers based on U_c has been dithered. Note that the RMSE values in the figure are expressed in degrees.

The flame model developed by Albini in the late 1970s and early 1980s [1, 18] has seen little validation and development since its introduction. To our knowledge, this is the 1st time that the parameters developed for chaparral fuels have been tested. Due to complex topography, changing fuel types, and the vagaries of local meteorology, a wildland fire is seldom an idealized line fire except in small segments. The limited agreement of the correlation by Yuan and Cox (Eq.(10)) with the chaparral fuel bed data indicates that there are still improvements that can be made. The chaparral fuel bed data were originally collected as part of a study examining marginal fire spread. Only about half of the fires which were ignited spread the entire length of the fuel bed. Several factors have been found to be related to fire spread success in these fuel beds; wind velocity was the most important [54]. These marginal conditions and the fact that the fuel beds were elevated resulting in additional entrainment may have contributed to the poor agreement with the data.

The strong relationship between mass loss rate and flame length in these live fuel beds extends this well-established relationship to these fuel types. The fitted exponent lends support to Byram's derivation that flame length is related to $Fr^{0.5}$ and not Thomas' derivation of $Fr^{2/3}$. Live foliage particles still retain significant moisture at the time of ignition [34, 35] indicating that the treatment of moisture and its transport in live fuel particles needs to be changed. The amount of water present in fuels may be an important parameter that should be included in these correlations if they are to be applied to live wildland fuels.

Acknowledgements

The measurements reported in this paper resulted from agreements between the USDA Forest Service, Pacific Southwest Research Station, Riverside, CA with Brigham Young University and the University of California-Riverside. The agreements were funded by the USDA/USDI National Fire Plan project 01.PSW.A.3 "Fire behavior in live fuels". The assistance of Dr. Arthur Pewsey, University of Extremadura with the circular-linear regression analysis and the comments of Dr. Ralph Nelson, Forest Service research (retired) regarding flame length and flame height are much appreciated.

References

[1] Albini, F.A., *Thermochemical properties of flame gases from fine wildland fuels*, INT-243, USDA Forest Service, Intermountain Forest and Range Experiment Station, Ogden, UT, (1980).

[2] Nelson, R.M., Jr., "An effective wind speed for models of fire spread," *Int. J. Wildland Fire* 11(2):153–161 (2002).

[3] Brown, J.K., Smith, J.K., *Wildland fire in ecosystems: effects of fire on flora*, RMRS-GTR-42-vol. 2, USDA Forest Service, Rocky Mountain Research Station, Fort Collins, CO (2000).

[4] Sandberg, D.V., Ottmar, R.D., Peterson, J.L., *Wildland fire in ecosystems: effects of fire on air*, RMRS-GTR-42-vol. 5, USDA Forest Service, Rocky Mountain Research Station, Fort Collins, CO (2002).

[5] Ryan, K.C., Jones, A.T., Koerner, C.L., Lee, K.M., *Wildland fire in ecosystems: effects of fire on cultural resources and archaeology*, RMRS-GTR-42-vol. 3, USDA Forest Service, Rocky Mountain Research Station, Fort Collins, CO (2012).

[6] Neary, D.G., Ryan, K.C., DeBano, L.F., *Wildland fire in ecosystems: effects of fire on soil and water*, RMRS-GTR-42-vol. 4, USDA Forest Service, Rocky Mountain Research Station, Fort Collins, CO (2005).
[7] Zouhar, K.L., Smith, J.K., Sutherland, S., Brooks, M.L., *Wildland fire in ecosystems: fire and nonnative invasive plants*, RMRS-GTR-42-vol. 6, USDA Forest Service, Rocky Mountain Research Station, Fort Collins, CO (2005).
[8] Smith, J.K., *Wildland fire in ecosystems: Effects of fire on fauna*, RMRS-GTR-42-vol. 1, USDA Forest Service, Rocky Mountain Research Station, Fort Collins, CO (2000).
[9] Butler, B.W., Cohen, J.D., "Firefighter safety zones: a theoretical model based on radiative heating," *Int. J. Wildland Fire* 8(2):73–77 (1998).
[10] Butler, B.W., "Wildland firefighter safety zones: a review of past science and summary of future needs," *Int. J. Wildland Fire* 23(3):295–308 (2014).
[11] Andrews, P.L., Rothermel, R.C., *Charts for interpreting wildland fire behavior characteristics*, INT-131, USDA Forest Service, Intermountain Forest and Range Experiment Station, Ogden, UT (1982).
[12] Drysdale, D., *An Introduction to Fire Dynamics (3rd ed)*, Wiley, Chichester, West Sussex (2011).
[13] Nelson, R.M., Jr., "In memory - George M. Byram - 1909-1996," *Int. J. Wildland Fire* 6(4): 216 (1996).
[14] Byram, G.M., "Scaling laws for modeling mass fires," *Pyrodynamics* 4:271–284 (1966).
[15] Byram, G.M., Martin, R.E., "Modeling of fire whirlwinds," *For. Sci.* 16(4):385–399 (1970).
[16] Byram, G.M., "Forest fire behavior," *Forest Fire : Control and Use*, K.P. Davis, ed., McGraw-Hill, New York, NY, 1959, pp. 89–123.
[17] Nelson, R.M., Jr., *Byram's energy criterion for wildland fires: units and equations*, INT-415, USDA Forest Service, Intermountain Research Station, Ogden, UT (1993).
[18] Albini, F.A., "A model for the wind-blown flame from a line fire," *Combust. Flame*, 43:155–174 (1981).
[19] Weise, D.R., Biging, G.S., "Effects of wind velocity and slope on flame properties," *Can. J. For. Res.* 26(10):1849–1858 (1996).
[20] Thomas, P.H., "Some aspects of the growth and spread of fire in the open," *Forestry* 40(2):139–164 (1967).
[21] Clark, T.L., Jenkins, M.A., Coen, J., Packham, D., "A coupled atmosphere-fire model: convective feedback on fire-line dynamics," *J. Appl. Meteorol.* 35:875–901 (1996).
[22] Zukoski, E.E., Kubota, T., Cetegen, B., "Entrainment in fire plumes," *Fire Saf. J.* 3(3):107–121 (1981).
[23] Yuan, L.-M., Cox, G., "An experimental study of some line fires," *Fire Saf. J.* 27(2):123–139 (1996).
[24] Nelson, R.M., Jr., *Flame characteristics for fires in southern fuels*, SE-RP-205, USDA Forest Service, Southeastern Forest Experiment Station, Asheville, NC (1980).
[25] Morvan, D., "Physical phenomena and length scales governing the behaviour of wildfires: a case for physical modelling," *Fire Technol.* 47(2):437–460 (2011).
[26] Morandini, F., Silvani, X., Rossi, L., Santoni, P.-A., Simeoni, A., Balbi, J.-H., Rossi, J.L., Marcelli, T., "Fire spread experiment across Mediterranean shrub: influence of wind on flame front properties," *Fire Saf. J.* 41(3):229–235 (2006).
[27] Morvan, D., "A numerical study of flame geometry and potential for crown fire initiation for a wildfire propagating through shrub fuel," *Int. J. Wildland Fire* 16(5):511–518 (2007).

[28] Morandini, F., Silvani, X., "Experimental investigation of the physical mechanisms governing the spread of wildfires," *Int. J. Wildland Fire* 19(5):570–582 (2010).
[29] Keeley, J.E., "Chaparral," *North American Terrestrial Vegetation*, M.G. Barbour and W.D. Billings, eds., Cambridge University Press, New York, NY, 2000, pp. 203–253.
[30] Cole, W.J., Dennis, M.H., Fletcher, T.H., Weise, D.R., "The effects of wind on the flame characteristics of individual leaves," *Int. J. Wildland Fire* 20(5):657-667 (2011).
[31] Sun, L., Zhou, X., Mahalingam, S., Weise, D.R., "Comparison of burning characteristics of live and dead chaparral fuels," *Combust. Flame* 144(1–2):349–359 (2006).
[32] Zhou, X., Weise, D., Mahalingam, S., "Experimental measurements and numerical modeling of marginal burning in live chaparral fuel beds," *Proc. Combust. Inst.* 30(2):2287–2294 (2005).
[33] Weise, D.R., Zhou, X., Mahalingam, S., Chong, J., *Marginal fire spread in live fuel beds - horizontal fuels*, RDS-2015-0007, USDA Forest Service Research Data Archive, Fort Collins, CO (2015).
[34] Fletcher, T.H., Pickett, B.M., Smith, S.G., Spittle, G.S., Woodhouse, M.M., Haake, E., Weise, D.R., "Effects of moisture on ignition behavior of moist California chaparral and Utah leaves," *Combust. Sci. Technol.* 179(6):1183–1203 (2007).
[35] Yashwanth, B.L., Shotorban, B., Mahalingam, S., Lautenberger, C.W., Weise, D.R., "A numerical investigation of the influence of radiation and moisture content on pyrolysis and ignition of a leaf-like fuel element," *Combust. Flame* 163:301–316 (2016).
[36] Engstrom, J.D., Butler, J.K., Smith, S.G., Baxter, L.L., Fletcher, T.H., Weise, D.R., "Ignition behavior of live California chaparral leaves," *Combust. Sci. Technol.* 176(9):1577–1591 (2004).
[37] Pickett, B.M., Isackson, C., Wunder, R., Fletcher, T.H., Butler, B.W., Weise, D.R., "Experimental measurements during combustion of moist individual foliage samples," *Int. J. Wildland Fire* 19(2):153–162 (2010).
[38] Pickett, B.M., Smith, S.G., Fletcher, T.H., Weise, D.R., "Burning characteristics of live California chaparral and Utah leaf samples," American Meteorological Society, Canmore, Alberta, Canada, 9 p., http://ams.confex.com/ams/pdfpapers/97573.pdf (2005).
[39] Zhou, X., Mahalingam, S., Weise, D., "Experimental study and large eddy simulation of effect of terrain slope on marginal burning in shrub fuel beds," *Proc. Combust. Inst.* 31(2):2547–2555 (2007).
[40] Weise, D.R., Koo, E., Zhou, X., Mahalingam, S., "A laboratory-scale comparison of rate of spread model predictions using chaparral fuel beds – preliminary results," *Proceedings of 3rd Fire Behavior and Fuels Conference*, D.D. Wade, M.L. Robinson, eds., International Association of Wildland Fire, Birmingham, AL, 17 p., https://www.fs.fed.us/psw/publications/weise/psw_2011_weise004.pdf (2011).
[41] Fons, W.L., Clements, H.B., George, P.M., "Scale effects on propagation rate of laboratory crib fires," 9th Symp. Int. Combust.:860–866 (1963).
[42] Thomas, P. H., "The size of flames from natural fires," 9th Symp. Int. Combust.:844–859 (1963).
[43] Zar, J. H., *Biostatistical Analysis (1st ed)*, Prentice-Hall, Englewood Cliffs, N.J., 1974, 620 p.
[44] Ferguson, S.C., Dahale, A., Shotorban, B., Mahalingam, S., Weise, D.R., "The role of moisture on combustion of pyrolysis gases in wildland fires," *Combust. Sci. Technol.* 185:435–453 (2013).

[45] Anderson, H.E., Rothermel, R.C., "Influence of moisture and wind upon the characteristics of free-burning fires," 10th Symp. Int. Combust.:1009–1019 (1965).
[46] Rothermel, R.C., Anderson, H.E., *Fire spread characteristics determined in the laboratory*, Res. Pap. INT-30, USDA Forest Service, Intermountain Forest and Range Experiment Station, Ogden, UT (1966).
[47] Mason, R.L., Gunst, R.F., Hess, J.L., *Statistical Design and Analysis of Experiments: with Applications to Engineering and Science*, Wiley, New York. 1989.
[48] Jammalamadaka, S.R., Sengupta, A., *Topics in Circular Statistics*, World Scientific, River Edge, N.J., 2001.
[49] Pewsey, A., Neuhäuser, M., Ruxton, G.D., *Circular Statistics in R*, Oxford University Press, Oxford ; New York. 2013.
[50] R Core Team, *R: A Language and Environment for Statistical Computing*, R Foundation for Statistical Computing, Vienna, Austria. 2015.
[51] Byram, G.M., "Combustion of forest fuels," *Forest Fire: Control and Use (1st ed)*, K.P. Davis, ed., McGraw-Hill, New York, 1959, pp. 61–89.
[52] Nelson, R.M., Jr. "Re-analysis of wind and slope effects on flame characteristics of Mediterranean shrub fires," *Int. J. Wildland Fire* 24(7):1001–1007 (2015).
[53] Pickett, B.M., "Effects of moisture on combustion of live wildland forest fuels," Ph.D. thesis, Brigham Young University, Provo, UT, 2008.
[54] Weise, D.R., Koo, E., Zhou, X., Mahalingam, S., Morandini, F., Balbi, J.-H., "Fire spread in chaparral - a comparison of laboratory data and model predictions in burning live fuels," *Int. J. Wildland Fire* 25(9):980–994 (2016).
[55] Mell, W., Maranghides, A., McDermott, R., Manzello, S.L., "Numerical simulation and experiments of burning Douglas fir trees," *Combust. Flame* 156(10):2023–2041 (2009).
[56] Zukoski, E., "Fluid dynamic aspects of room fires," 1st Fire Saf. Sci.:1–30 (1986).
[57] Hasemi, Y., Nishihata, M., "Fuel shape effect on the deterministic properties of turbulent diffusion flames," 2nd Fire Saf. Sci.:275–284 (1989).
[58] Nelson, R.M., Jr., Butler, B.W., Weise, D.R., "Entrainment regimes and flame characteristics of wildland fires," *Int. J. Wildland Fire* 21(2):127–140 (2012).
[59] Eisenhauer, J.G. "Regression through the origin," *Teaching Statistics* 25(3):76–80 (2003).
[60] Padhi, S., Shotorban, B., Mahalingam, S., "Computational investigation of flame characteristics of a non-propagating shrub fire," *Fire Saf. J.* 81:64–73 (2016).
[61] Li, J., Mahalingam, S., Weise, D.R., "Experimental investigation of fire propagation in single live shrubs," *Int. J. Wildland Fire* 26(1): 58–70 (2017).